Proc. Estonian Acad. Sci. Phys. Math., 2003, **52**, 3, 257–265
https://doi.org/10.3176/phys.math.2003.3.02

High-temperature atomic layer epitaxy of TiO_2 from $TiCl_4$ and H_2O_2–H_2O

Ahti Niilisk, Arnold Rosental, Aivar Tarre, and Teet Uustare

Institute of Physics, University of Tartu, Riia 142, 51014 Tartu, Estonia; niilisk@fi.tartu.ee

Received 20 January 2003, in revised form 10 March 2003

Abstract. Epitaxial TiO_2 films were grown on off-cut α-$Al_2O_3(0\,1\,\bar{1}\,2)$ (*R*-plane sapphire) substrates by gas-phase atomic layer deposition at 550–750 °C. X-ray diffraction and reflection high-energy electron diffraction measurements showed that the films had a two-domain $(1\,0\,1)$ textured rutile structure. The domains made a straight angle about the normal to the substrate $(0\,1\,\bar{1}\,2)$ plane; those quantitatively superior were 3° inclined with respect to the plane, resulting in the overall orientation relationship $(0\,1\,\bar{1}\,2)[2\,\bar{1}\,\bar{1}\,0]_{\text{sapphire}} \parallel (1\,0\,1)[0\,1\,0],[0\,\bar{1}\,0]\,(3°)_{\text{rutile}}$. An account of the two-domain growth was given. The epitaxial quality worsened with the increase in the deposition temperature.

Key words: atomic layer deposition, epitaxy, rutile titanium dioxide, *R*-plane sapphire, X-ray diffraction, X-ray fluorescence, reflection high-energy electron diffraction.

1. INTRODUCTION

Single-crystal α-$Al_2O_3(0\,1\,\bar{1}\,2)$ has been used on numerous occasions as a substrate for epitaxial deposition of thin films. There are $(1\,\bar{1}\,0\,2)$ and $(\bar{1}\,0\,1\,2)$ structural equivalents, and the product is frequently referred to as *R*-plane sapphire. The heterocompositions obtained are of great concern by themselves and for various applications. Interestingly, the list of materials that can be epitaxially deposited on *R*-plane sapphire is rather long. It includes, e.g., AlN [1], Al_2O_3 [2] (homoepitaxy), $Bi_4Ti_3O_{12}$ [3], CdTe [4], CeO_2 [5], $Cu_2Mo_6S_8$ [6], $EuAlO_3$ [7], $GdAlO_3$ [8], GaAs [9], GaN [10], Ge [11], MgO [12], Nb [13], Si [14], SnO_2 [15], $SrTiO_3$ [16], VO_2 [17], WO_3 [18], $YBa_2Cu_3O_{7-\delta}$ [19], ZnO [20], and ZrO_2 [21]. TiO_2 ranks rather high on the list [22–30]. Works [25–27,30] are relevant to the growth of TiO_2 on the *R*-sapphire substrates by gas-phase atomic layer deposition (ALD) [31,32]. When performing ALD, TiI_4–H_2O, TiI_4–H_2O_2, TiI_4–O_2, and $TiCl_4$–H_2O precursor combinations have been used. Irrespective of the

combination, the crystalline quality of the ALD-grown films has been shown to increase with deposition temperature, T_{dep}. In previous studies, the temperature, however, did not exceed the 500 °C limit.

The objective of the present experiments was to determine the crystal characteristics of titanium dioxide films, ALD-grown on the *R*-plane sapphire substrates at temperatures higher than those used to date. In the experiments, the range of T_{dep} was extended to 750 °C. Multiple domain structure of the films and crystallographic tilting of the domains were studied.

2. EXPERIMENTAL

We grew TiO_2 films onto single-crystalline 0.5° off-oriented α-Al_2O_3 $(0\,1\,\bar{1}\,2)$ substrates in a self-constructed miniature travelling-wave ALD reactor from silica with a channel cross-section of 30 mm^2 [33]. The surface area of the substrates was 100 mm^2. Prior to being placed into the reactor, they were boiled in a mixture of H_2SO_4, H_2O_2, and H_2O, and rinsed in triple distilled water. The source materials, 99.9%-pure $TiCl_4$ and a 30% aqueous solution of H_2O_2, were evaporated at 26 °C. N_2 of 99.999% purity was used as a carrying, supply switching, and purging gas. The total gas flow rate was 80 sccm. The vacuum in the reactor was held at 10 mbar. A deposition cycle included a 0.2 s $TiCl_4$ supply, 0.3 s purge, 1 s H_2O_2–H_2O supply, and 1 s purge. In a growth-run, 100–3000 cycles were applied. Deposition temperature varied from 550 to 750 °C.

The quality of the product films was examined by X-ray diffraction (XRD) and reflection high-energy electron diffraction (RHEED), their thickness, by X-ray fluorescence (XRF) along with the calibration by X-ray reflection (XRR). In carrying out these experiments, use was made of D 5000 (Bruker AXS) and X'Pert MRD (PANalytical) X-ray diffractometers with Cu K_α tube sources, a X-Lab 2000 (Spectro AI) X-ray fluorescence spectrometer measuring Ti K_α signal, and an EMR-100 electron diffractometer providing depth information from several nanometres underneath the sample surface. The XRD data were obtained upon adjusting the substrate $(0\,1\,\bar{1}\,2)$ plane parallel to the holder surface. Low- (1°) and high-angle incidence was used, as well as a variation of four standard positioning angles: 2θ, ω (θ-rocking), φ (azimuth), and ψ (tilt). The 2θ-signal was measured under continuous φ-rotation. On the analogy of [34], the film thickness was *in situ* assessed by registering the Brewster-angle reflection-geometry optical interference signal (light source 633 nm He–Ne laser) from the film depositing on the inner side of a quartz-glass window-substrate – a constituent part of the reactor – substituted together with the sapphire substrate.

3. RESULTS AND DISCUSSION

The *ex situ* XRF–XRR measurements demonstrated that the growth rate of TiO_2 films (Fig. 1), decreasing linearly with the T_{dep} increase, was considerably

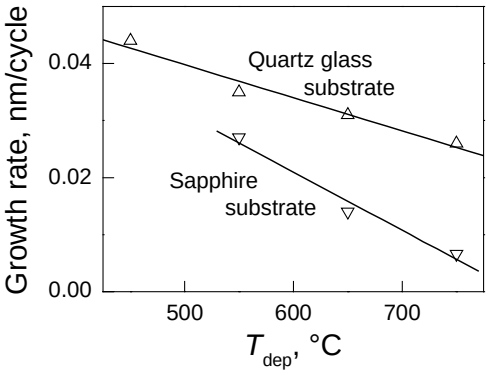

Fig. 1. XRF–XRR determined T_{dep} dependences of ALD rate of TiO_2 on *R*-sapphire and amorphous quartz substrates. In the latter case the deposit was a polycrystalline anatase–rutile mixture.

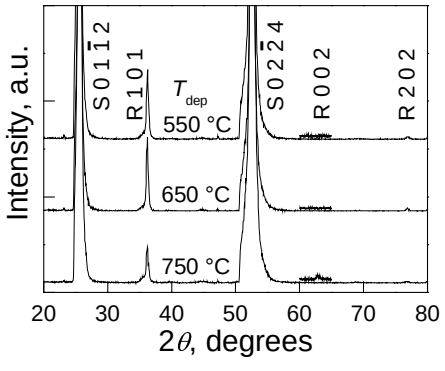

Fig. 2. XRD θ–2θ-scans for TiO_2 films, ALD grown on *R*-sapphire substrates at different T_{dep}. The 550, 650, and 750 °C films were respectively 56, 39, and 8 nm thick. R stands for rutile, S for sapphire.

slower on single-crystalline *R*-plane sapphire than on amorphous window-quartz, taken as a reference; a quicker decrease was likewise characteristic of deposit formation on sapphire (the rate equalled 0.027 and 0.006 nm per cycle at 550 and 750 °C, respectively). The small and unsaturated gain suggests that the realized process was, in fact, far from true ALD.

Figure 2 shows XRD θ–2θ-scans of the samples prepared. On the scans, diffraction peaks indexable as TiO_2 (rutile) $1\,0\,1$ and $2\,0\,2$ can be easily observed. Thus, the films deposited on α-Al_2O_3 $(0\,1\,\bar{1}\,2)$ substrates were monophasic and strongly $1\,0\,1$ oriented. Accordingly, the out-of-plane orientation relationship was $(0\,1\,\bar{1}\,2)_{\text{sapphire}} \parallel (1\,0\,1)_{\text{rutile}}$. Yet, as follows from the grazing incidence scans short cuts of which complete the set of the plots depicted in Fig. 2, a small amount of $0\,0\,2$ domains tilted relative to the $(1\,0\,1)$ plane appeared in a film prepared at the highest T_{dep}.

Rather low values, not exceeding 1°, of the full width at half-maximum (FWHM) of ω-scans (Fig. 3) are indicative of an epitaxy with a medium-grade out-of-plane alignment. The highest-temperature films had, with their 1° FWHM, the most pronounced mosaic spread.

X-ray diffractometry φ-scans were used to identify the in-plane orientation relationship. Note that the number of peaks in a φ-scan shows the number of crystallographic planes of a particular family that form the same angle with the surface plane, or, substitutionally, with the immediately adjacent high-atom-population plane. In our case, the $(0\,1\,\bar{1}\,2)$ plane of the substrate and the $(1\,0\,1)$ plane of the film served as reference planes. The lower curve in Fig. 4 shows a result of φ-scanning for the sapphire $\{0\,2\,\bar{2}\,10\}$ family. There is only one plane out of six, namely $(0\,2\,\bar{2}\,10)$, which has an angle of 25.38° (calculated value) with the reference plane. In consequence, a single peak should be seen, just as on the curve. Since φ was scanned with steps of 0.5°, they were, due to a high quality of the substrates, too large to give an estimate of the width of the peak.

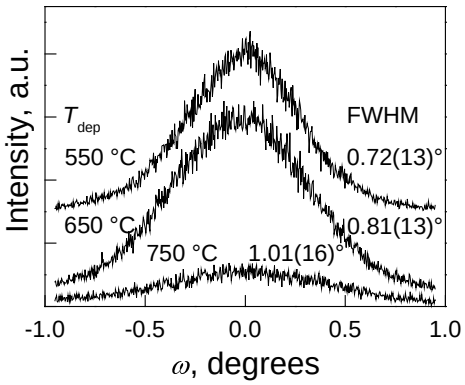

Fig. 3. XRD ω-scans for TiO_2 films, ALD grown on *R*-sapphire substrates at different T_{dep}. The samples were the same as in Fig. 2.

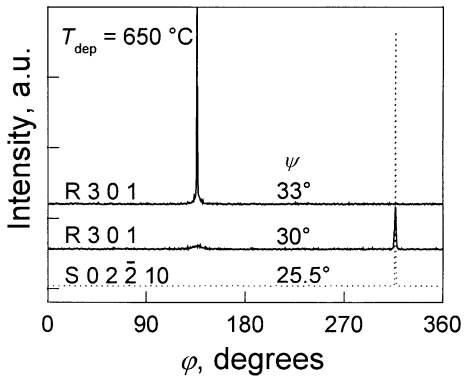

Fig. 4. XRD φ-scans obtained at different sample tilt angles ψ for the $0\,2\,\bar{2}\,10$ reflection from a *R*-sapphire substrate and the $3\,0\,1$ reflection from a 39 nm TiO_2 film ALD grown at 650 °C. R and S denote rutile and sapphire, respectively.

The middle curve in Fig. 4 is a φ-scan for the TiO_2 rutile $\{3\,0\,1\}$ family. There is only one plane out of four, namely $(3\,0\,1)$, which makes an angle of 29.85° with the reference plane. Again, only one peak should appear. The peak present on the curve near 315° meets the expectations. It has a FWHM of about 2°, implying quite a high in-plane alignment of the film. The peak occupies the same φ position as that of sapphire $(0\,2\,\bar{2}\,10)$. Thus, because the zone axis for the sapphire $(0\,1\,\bar{1}\,2)$ and $(0\,2\,\bar{2}\,10)$ planes is $[2\,\bar{1}\,\bar{1}\,0]$ and that for the rutile $(1\,0\,1)$ and $(3\,0\,1)$ planes is $[0\,1\,0]$, the in-plane epitaxial relationship was $[2\,\bar{1}\,\bar{1}\,0]_{\text{sapphire}} \| [0\,1\,0]_{\text{rutile}}$.

This in-plane relationship was, however, neither unique nor dominant. Note, first, that instead of one peak expected for a single-domain TiO_2 film, two peaks were seen, the second being shifted by 180°. On the middle curve, the shifted, left-positioned peak is rather small. The appearance of the two peaks verifies the coexistence of two domains having a 180° in-plane rotation. Further, the ψ-tilting of the sample could increase the left-hand peak. Shown in Fig. 4 (upper curve) is the φ-scan of the film obtained by changing the tilt angle by $\Delta\psi = 3°$, which brought the intensity of the peak to an upper limit. The maximum observed exceeded the maximum of the other peak it had at $\Delta\psi = 0°$. The widths of both peaks were equal (FWHM ~ 2°). Thus, the quantitative prevalence of the domains, characterized by a slight inclination of the $(1\,0\,1)$ plane with respect to the substrate $(0\,1\,\bar{1}\,2)$ plane and their straight-angle rotation compared to the "regular" orientation, has been established. A generalized orientation relationship for these domains can be written as $[2\,\bar{1}\,\bar{1}\,0]_{\text{sapphire}} \| [0\,\bar{1}\,0](3°)_{\text{rutile}}$.

The competition between the two domains might be understood by looking at the diagrammatic presentations of the atomic arrangement on the cross-sections of the interface between the film and substrate (Fig. 5a,b). For both materials, the

arrangement, which is shown, copies that of the bulk. Here it is not necessary to go over the arrangements on the $(0\,1\,\bar{1}\,2)$ plane of sapphire and $(1\,0\,1)$ plane of rutile titanium dioxide: their schematics can be found in a number of articles (see, e.g., [25]). It should, however, be noted that, judging by the schematics, the surface-plane fit-together of oxygen sublattices, imperfect as it is, worsens remarkably when rutile is rotated by 180°. Being of the opinion that in our case it is easier to estimate the fit/unfit by examining cross-sectional positions of the atoms, we have calculated them. An assumption was made that the growth begins with the filling of Al sites by Ti (cf. [35,36]). Figure 5a shows that in the "regular" case the atomic network continues not very much perturbed across the sapphire–rutile interface. If the other domains were only rotated about the normal to the $(1\,0\,1)$ plane, it would not be the case. A corresponding cross-sectional view (not shown here) provides the proof. On the other hand, the inclination of the latter domains can restore, to a high degree, the quality of the continuation of the atomic network (Fig. 5b). Hence the growth of the rotated-inclined domains in parallel to the regular ones should be rather probable. The existence of the two-domain structure in fairly thick (~60 nm) films might be explained by the columnar or lamellar growth of the domains.

The RHEED images for the 8 nm films grown at 650 and 750 °C are depicted in Fig. 6a,b. Both images demonstrate that the growth of the films took place in a three-dimensional mode. Continuing from 550 °C (the pattern is not shown), the

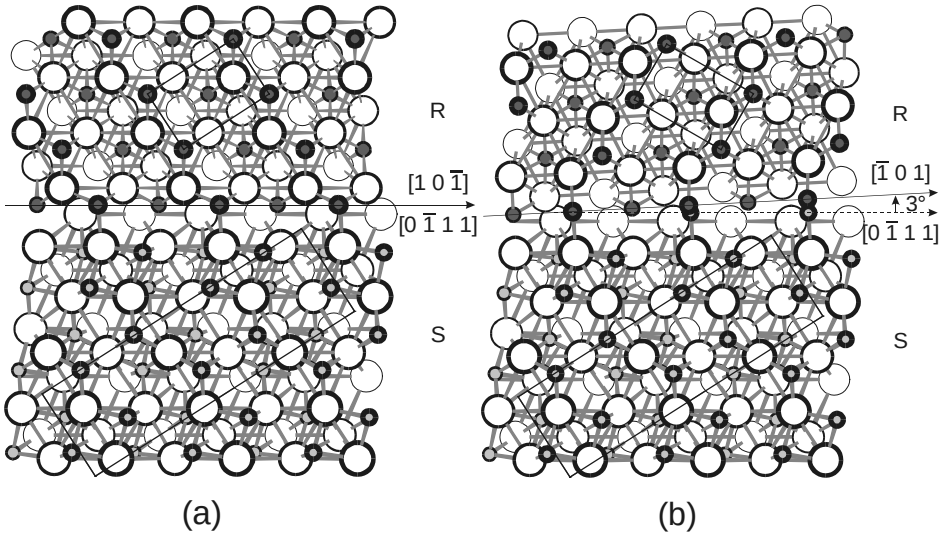

Fig. 5. Cross-sectional schematics of atomic arrangement at the interface between rutile $TiO_2\,(1\,0\,1)$ and α-$Al_2O_3\,(0\,1\,\bar{1}\,2)$ for (a) untilted (view along $[0\,1\,0]$) and (b) tilted (view along $[0\,\bar{1}\,0]$) domains in the film. Shown are parallel layers: two consisting of Ti atoms (dark circles), two of Al atoms (light circles), and four of O atoms (large circles), the more inward, the thinner is the contouring. Rectangles are outlines of the rutile (R) tetrahedral and sapphire (S) hexagonal unit cells projected onto the cross-sectional planes $(0\,1\,0)$ and $(\bar{2}\,1\,1\,0)$, respectively.

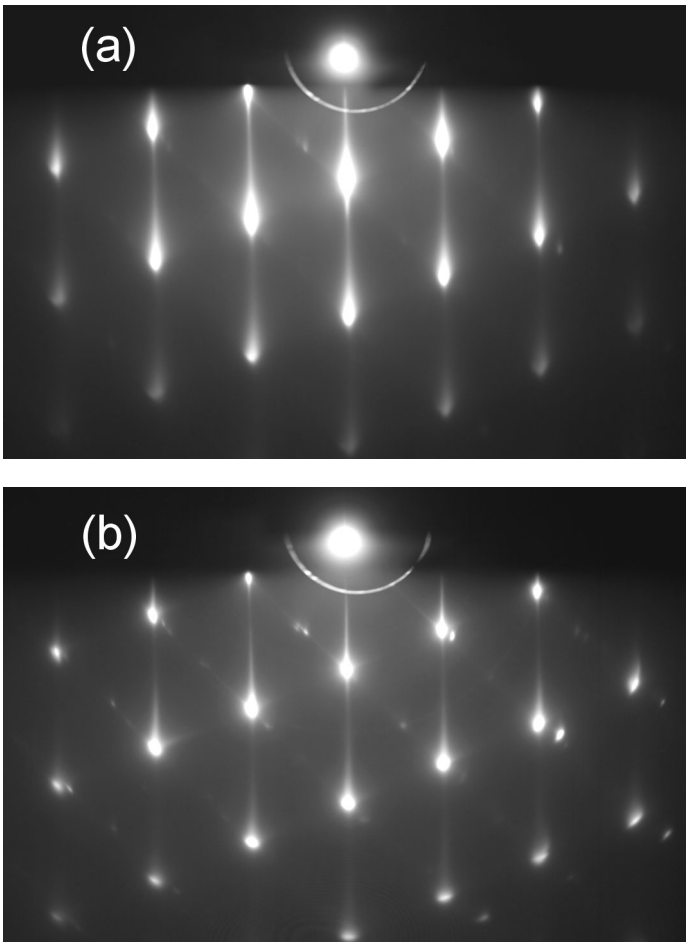

Fig. 6. RHEED images for 8 nm TiO_2 films, ALD grown at (a) 650 and (b) 750 °C on *R*-sapphire substrates.

diffraction features gradually lost their streakiness. The loss reflects the increase in the islanding-caused microroughness of the films with T_{dep}. A superimposed ring pattern, although hardly visible in Fig. 6b, almost total absence of the spot elongation, deformation of peripheral features, and appearance of new, abnormal spots were characteristic of the 750 °C films. All this proves, like XRD data did, that these films had the worst epitaxial quality.

A more detailed study of the formation of the domain structure at issue is yet to be made. It is of interest, e.g., to determine whether the phenomenon is connected with the inclination of the substrate and if so, how the angle and direction of this inclination change the result. Application of the cross-sectional high-resolution transmission electron microscopy in the analysis would also be of great interest.

4. CONCLUSIONS

Epitaxial TiO_2 rutile films were ALD-grown in a high-temperature range of 550–750 °C. The growing was performed from $TiCl_4$ and H_2O_2–H_2O on 0.5° off-axis *R*-plane sapphire. The films were (1 0 1) textured and exhibited a two-domain structure. Some domains were rotated relative to the others through 180° about the normal to the substrate $(0\,1\,\bar{1}\,2)$ plane. The quantitatively superior domains were, in addition, inclined by 3° with respect to this plane. Briefly, the crystallographic relationship $(0\,1\,\bar{1}\,2)[2\,\bar{1}\,\bar{1}\,0]_{\text{sapphire}} \parallel (1\,0\,1)[0\,1\,0],[0\,\bar{1}\,0](3°)_{\text{rutile}}$ held. A possible explanation for the two-domain growth was offered. In the range of interest, the epitaxial quality of the films was found to worsen with an increase in T_{dep}.

ACKNOWLEDGEMENTS

The authors gratefully acknowledge the financial support from the Estonian Science Foundation (grant No. 4205). The post-growth experiments were partially performed in the Ångström Laboratory of Uppsala University. One of us (A. T.) thanks the Royal Swedish Academy of Sciences and Uppsala University for granting his work in the laboratory and Dr. Mikael Ottosson for his help in the application of the X'Pert XRD system.

REFERENCES

1. Shibata, T., Asai, K., Nakamura, Y., Tanaka, M., Kaigawa, K., Shibata, J. and Sakai, H. AlN epitaxial growth on off-angle *R*-plane sapphire substrates by MOCVD. *J. Cryst. Growth*, 2001, **229**, 63–68.
2. Oya, G. and Sawada, Y. Molecular layer epitaxy of α-Al_2O_3 films. *J. Cryst. Growth*, 1990, **99**, 572–576.
3. Masumoto, H., Goto, T., Masuda, Y., Baba, A. and Hirai, T. Preparation of $Bi_4Ti_3O_{12}$ films on a single-crystal sapphire substrate with electron cyclotron resonance plasma sputtering. *Appl. Phys. Lett.*, 1991, **58**, 243–245.
4. Kasuga, M., Futami, H. and Iba, Y. Vapor phase epitaxy of CdTe on sapphire and GaAs. *J. Cryst. Growth*, 1991, **115**, 711–717.
5. Chromik, Š., Cannaerts, M., Gaži, Š., Van Haesendonck, C., Španková, M., Kúš, P. and Beňačka, Š. The influence of $(1\,\bar{1}\,0\,2)$ sapphire substrate on structural perfection of CeO_2 thin films. *Physica C*, 2002, **371**, 301–308.
6. Lemee, N., Guilloux-Viry, M., Perrin, A. and Sergent, M. Superconducting $Cu_2Mo_6S_8$ thin films deposited in-situ by laser ablation on *R*-plane sapphire. *Eur. Phys. J. – Appl. Phys.*, 1988, **1**, 197–201.
7. Yamaguchi, I., Manabe, T., Sohma, M., Tsuchiya, T., Yamaguchi, Y., Suzuki, S., Kumagai, T. and Mizuta, S. Preparation of $YBa_2Cu_3O_{7-x}$/$EuAlO_3$ multilayer films on α-Al_2O_3 substrates by all-coating-pyrolysis process. *Physica C*, 2002, **382**, 269–275.
8. Senz, S., Sieber, H., Zakharov, N. D., Lorenz, M., Hochmuth, H. and Hesse, D. Sputtered and reactively grown epitaxial $GdAlO_3$ films as buffer layers for C-oriented $YBa_2Cu_3O_{7-\delta}$ films on R-sapphire. *Mater. Res. Soc. Symp. Proc.*, 1996, **401**, 357–362.

9. Chin, A., Bhattacharya, P., Chang, K. H. and Biswas, D. Optical and structural properties of molecular-beam epitaxial GaAs on sapphire. *J. Vac. Sci. Technol. B*, 1989, **7**, 283–288.
10. Craven, M. D., Lim, S. H., Wu, F., Speck, J. S. and DenBaars, S. P. Structural characterization of nonpolar $(11\bar{2}0)$ *a*-plane GaN thin films grown on $(1\bar{1}02)$ *r*-plane sapphire. *Appl. Phys. Lett.*, 2002, **81**, 469–471.
11. Godbey, D. J., Qadri, S. B., Twigg, M. E. and Richmond, E. D. Single-crystal germanium grown on $(1\bar{1}02)$ sapphire by molecular beam epitaxy. *Appl. Phys. Lett.*, 1989, **54**, 2449–2451.
12. Stampe, P. A., Bullock, M., Tucker, W. P. and Kennedy, R. J. Growth of MgO thin films on *M*-, *A*-, *C*- and *R*-plane sapphire by laser ablation. *J. Phys. D*, 1999, **32**, 1778–1787.
13. Delaët, B., Feautrier, P., Petmezakis, P., Villégier, J.-C., Benoit, A. and Bret, J.-L. Optical and near-infrared photon counting detector using superconducting tunnel junctions. *Nucl. Instr. and Meth. A*, 2000, **444**, 465–468.
14. Abrahams, M. S., Hutchison, J. L. and Booker, G. R. Direct observation of a silicon-sapphire hetero-epitaxial interface by high resolution transmission electron microscopy. *Phys. Stat. Sol. A*, 1981, **63**, K3–K6.
15. Tarre, A., Rosental, A., Aidla, A., Aarik, J., Sundqvist, J. and Hårsta, A. New routes to SnO_2 heteroepitaxy. *Vacuum*, 2002, **67**, 571–575.
16. Char, K., Newman, N., Garrison, S. M., Barton, R. W., Taber, R. C., Laderman, S. S. and Jacowitz, R. D. Microwave surface resistance of epitaxial $YBa_2Cu_3O_7$ thin films on sapphire. *Appl. Phys. Lett.*, 1990, **57**, 409–411.
17. Chang, H. L. M., You, H., Parker, J. C., Guo, J., Gao, Y. and Lam, D. J. Ceramic epitaxial films and multilayers prepared by MOCVD. In *High Performance Ceramic Films and Coatings* (Vincenzini, P., ed.). Elsevier, Amsterdam, 1991, 161–170.
18. Garg, A., Leake, J. A. and Barber, Z. H. Epitaxial growth of WO_3 films on $SrTiO_3$ and sapphire. *J. Phys. D*, 2000, **33**, 1048–1053.
19. Young, R. T., Young, K. H., Muller, M. D., Ovshinsky, S. R., Budai, J. D., White, C. W. and Martens, J. S. High quality epitaxial YBCO(F) films directly deposited on sapphire. *Physica C*, 1992, **200**, 437–441.
20. Zhang, B. P., Segawa, Y., Wakatsuki, K., Kashiwaba, Y. and Haga, K. Structural and optical properties of ZnO films grown on *R*-Al_2O_3 substrates. *Appl. Phys. Lett.*, 2001, **79**, 3953–3955.
21. Moulzolf, S. C., Yu, Y., Frankel, D. J. and Lad, R. J. Properties of ZrO_2 films on sapphire prepared by cyclotron resonance oxygen-plasma-assisted deposition. *J. Vac. Sci. Technol. A*, 1997, **15**, 1211–1214.
22. Chen, S., Mason, M. G., Gysling, H. J., Paz-Pujalt, G. R., Blanton, T. N., Castro, T., Chen, K. M., Fictorie, C. P., Gladfelter, W. L., Franciosi, A., Cohen, P. I. and Evans, J. F. Ultrahigh vacuum metalorganic chemical vapor deposition growth and *in situ* characterization of epitaxial TiO_2 films. *J. Vac. Sci. Technol. A*, 1993, **11**, 2419–2429.
23. Fukushima, K., Takaoka, G. H. and Yamada, I. Epitaxial growth of TiO_2 rutile thin films on sapphire substrates by a reactive ionized cluster beam method. *Jpn. J. Appl. Phys.*, 1993, **32**, 3561–3565.
24. Gao, Y., Thevuthasan, S., McCready, D. E. and Engelhard, M. MOCVD growth and structure of Nb- and V-doped TiO_2 films on sapphire. *J. Cryst. Growth*, 2000, **212**, 178–190.
25. Schuisky, M., Hårsta, A., Aidla, A., Kukli, K., Kiisler, A.-A. and Aarik, J. Atomic layer chemical vapor deposition of TiO_2: low temperature epitaxy of rutile and anatase. *J. Electrochem. Soc.*, 2000, **147**, 3319–3325.
26. Aarik, J., Aidla, A., Mändar, H., Uustare, T., Schuisky, M. and Hårsta, A. Atomic layer growth of epitaxial TiO_2 thin films from $TiCl_4$ and H_2O on α-Al_2O_3 substrates. *J. Cryst. Growth*, 2002, **242**, 189–198.
27. Aarik, J., Aidla, A., Uustare, T., Kukli, K., Sammelselg, V., Ritala, M. and Leskelä, M. Atomic layer deposition of TiO_2 thin films from TiI_4 and H_2O. *Appl. Surf. Sci.*, 2002, **193**, 277–286.

28. Huang, J. Y., Park, B. H., Jan, D., Pan, X. Q., Zhu, Y. T. T. and Jia, Q. X. High-resolution transmission electron microscopy study of defects and interfaces in epitaxial TiO_2 films on sapphire and $LaAlO_3$. *Phil. Mag. A*, 2002, **82**, 735–749.
29. Park, B. H., Huang, J. Y., Li, L. S. and Jia, Q. X. Role of atomic arrangements at interfaces on the phase control of epitaxial TiO_2 films. *Appl. Phys. Lett.*, 2002, **80**, 1174–1176.
30. Schuisky, M., Kukli, K., Aarik, J., Lu, J. and Hårsta, A. Epitaxial growth of TiO_2 films in a hydroxyl-free atomic layer deposition process. *J. Cryst. Growth*, 2002, **235**, 293–299.
31. Suntola, T. Atomic layer epitaxy. In *Handbook of Crystal Growth*, Vol. 3 (Hurle, D. T. J., ed.). Elsevier, Amsterdam, 1994, 601–663.
32. George, S. M., Ott, A. W. and Klaus, J. W. Surface chemistry for atomic layer growth. *J. Phys. Chem.*, 1996, **100**, 13121–13131.
33. Niilisk, A., Rosental, A., Gerst, A., Sammelselg, V. and Uustare, T. Atomic-scale optical monitoring of the initial growth of TiO_2 thin films. In *Smart Optical Inorganic Structures and Devices* (Ašmontas, S. P. and Gradauskas, J., eds.). *Proc. SPIE*, 2001, **4318**, 72–77.
34. Niilisk, A., Rosental, A., Uustare, T., Kasikov, A. and Tarre, A. Chloride atomic-layer chemical vapor deposition of TiO_2 with a chloride pretreatment of substrates. *J. Phys. IV*, 2001, **11**, 103–107.
35. Nolder, R. and Cadoff, I. Heteroepitaxial silicon–aluminium oxide interface. Part II – Orientation relations of single-crystal silicon on alpha aluminium oxide. *Trans. Met. Soc. AIME*, 1965, **233**, 549–556.
36. Dominguez, J. E., Pan, X. Q., Fu, L., Van Rompay, P. A., Zhang, Z., Nees, J. A. and Pronko, P. P. Epitaxial SnO_2 thin films grown on $(\bar{1}012)$ sapphire by femtosecond pulsed laser deposition. *J. Appl. Phys.*, 2002, **91**, 1060–1065.

TiO_2 kõrgematemperatuurne aatomkihtepitaksia $TiCl_4$ ja H_2O_2–H_2O-st

Ahti Niilisk, Arnold Rosental, Aivar Tarre ja Teet Uustare

Kasutades menetlusena gaasifaas-aatomkihtsadestamist ja alusmaterjalina vitsinaalset α-Al_2O_3 $(01\bar{1}2)$ (*R*-safiir), realiseeriti töötemperatuuril 550–750 °C TiO_2 kilede kasvatamine epitaksiaalvormis. Röntgendifraktsiooni ja peegeldunud suure energiaga elektronide difraktsiooni mõõtmised näitasid, et protsessi resultaat oli kahedomeeniline (1 0 1)-tekstureeritud rutiil. Domeenid paiknesid sirgnurgi aluse $(01\bar{1}2)$-pinna normaali ümber; need domeenid, mis olid arvulises ülekaalus, olid 3° kaldu selle pinna suhtes. Kokku võttes kehtis orientatsioonisuhe $(01\bar{1}2)[2\bar{1}\bar{1}0]_{safiir} \parallel (101)[010],[0\bar{1}0](3°)_{rutiil}$. Pakuti välja kahedomeenilise kasvu seletus. Sadestustemperatuuri tõstmisel kilede epitaksiaalomadused halvenesid.